Journal of Zhejiang University SCIENCE A
ISSN 1673-565X (Print); ISSN 1862-1775 (Online)
www.zju.edu.cn/jzus; www.springerlink.com
E-mail: jzus@zju.edu.cn

Cyclic behavior test of a new double-arch steel gate*

LUO Yao-zhi[1], ZHU Shi-zhe[†‡1,2], CHEN Xi[1]

([1]*Space Structures Research Center, Zhejiang University, Hangzhou 310027, China*)

([2]*School of Landscape Architecture and Art, Zhejiang Forestry University, Hangzhou 311300, China*)

[†]E-mail: zhushizhe@163.com

Received Dec. 19, 2006; revision accepted Mar. 21, 2007

Abstract: A new double-arch structure for the gate used as tidal barrage and sluice was adopted in Caoe River Dam in China. It was a spatial structure made up of the right arch, the invert arch, the chord, etc., and was designed to bear bilateral loads. To research the cyclic behavior of the new double-arch structure, a scale-model cyclic test was conducted. First, the test setup and test method were presented in detail, and according to the test results, the cyclic behavior and failure characteristics of this structure were discussed. Then by analyzing the test cyclic envelope curve, it was found the curve was divided into three stages: the elastic stage, the local plastic stage and the failure stage at the local yield point and structural yield point. The gate model has local yield strength and structural yield strength, with both their values being bigger than that of the designing load. Therefore, the gate is safe enough for the projects. At last, dynamic property of the gate was analyzed considering additional mass of the water. It was found that the tidal bore shock would not cause resonance vibration of the gate.

Key words: Double-arch steel gate, Cyclic behavior test, Cyclic envelope curve, Dynamic property
doi:10.1631/jzus.2007.A1731 **Document code:** A **CLC number:** TV3; TU3

INTRODUCTION

Spatial structures using hollow steel tubes as main load-bearing members have been widely used in large-span structures (e.g. stadiums and bridges), because of their high rigidity, good hydrodynamic characteristics, aesthetic shape and reduced steel consumption (Dong *et al.*, 2003). However, it is hardly ever used for hydraulic steel gates.

This paper introduces a new double-arch steel gate whose loading-bearing structure is made up of double-arch structures. As a spatial structure, it inherits the advantages of spatial structures, that is, the members mainly bear axial stress. It has high rigidity and large load-bearing capacity compared with the traditional gate made up of solid wed girder with most of its members bearing bending stress. As a result, this new gate can save about 30%~50% steel consumption under the same condition (Zhu, 2005).

The new gate is used in the Caoe River Dam as tidal barrage and sluice. Caoe River Dam is located at Caoe River estuary on the south bank of Qiantang River in Zhejiang Province, China. Renowned as 'the first estuary Dam in China', it has a total of 28 gates, each 21.2 m in length and 5 m in height. As the gate is subject to bilateral loads of water pressure on the Caoe River side of the gates and tidal bore stroke on the Qiantang River side, a double-arch structure including the right arch, invert arch, chord and web members was designed (Fig.1). The entire gate consists of four double-arch structures with the face plate being welded on the chords directly (Fig.2). The tidal bore shock on the Qiantang River side is the main load and regarded as a uniform load on the gate. The designed value of it reaches 98 kN/m^2 and the total load on the gate is 10^4 kN.

The double-arch steel gate is a new type of gate and it is the first application in hydraulic project. Moreover, during the long service life the loads acting on gate are very complex (such as special tidal bore

‡ Corresponding author

* Project supported by the Research Foundation for the Doctoral Program of Higher Education of China (No. 20050335097) and Caoe River Dam Investment Ltd., China

shock in the Qiantang River, extraordinary typhoon, earthquake and ship crash). Therefore, an experimental investigation on the double-arch steel gate is necessary. In this way, the damage, cyclic behavior, strength, and ductility of the gate can be observed. Moreover, the dynamic property of the gate is also analyzed.

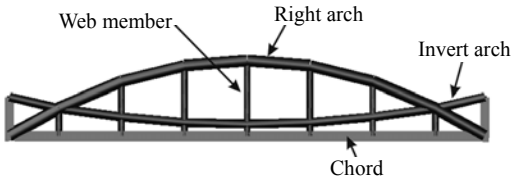

Fig.1 A piece of the double-arch structure

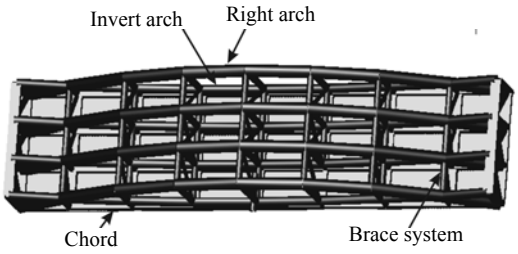

Fig.2 Structure of the double-arch steel gate

So far a number of experimental researches on gate have been conducted (Ead and Rajaratnam, 1998; Billeter and Staubli, 2000; Mostafiz and Robert, 1996), but most of them focused on the vibration of the gate. Though some studies on the property of steel structures under cyclic load by experiments have been conducted (Hsu and Shyu, 2001; Kleiser, 1999; Elchalakani *et al.*, 2003; Lin *et al.*, 1970; Alinia and Dastfan, 2007), most of them focus on the structural members, not the entire structure. Cyclic tests on the entire steel structures are seldom reported in particular. This paper is aimed: (1) to study the cyclic behavior of this new gate by simulating the uniform bilateral load of the gate; (2) to research the bearing capacity characteristics of this new gate according to the cyclic envelope curve; and (3) to research the dynamic property considering the additional mass of the water.

TEST SETUP AND LOADING PLAN

Test model and test setup

The dimension of the full-scale gate was 21.2 m×5.0 m. The test model was a 1/8-scale model of the full-scale gate (Fig.3). It was designed to resemble the full-scale gate in geometry. The cross-section of the member was scaled according to the similarity principle. It was ensured that the test model would have similar response as the ideal 1/8-scale model. The cross-sections of the members of the model are listed in Table 1 and the materials used are listed in Table 2.

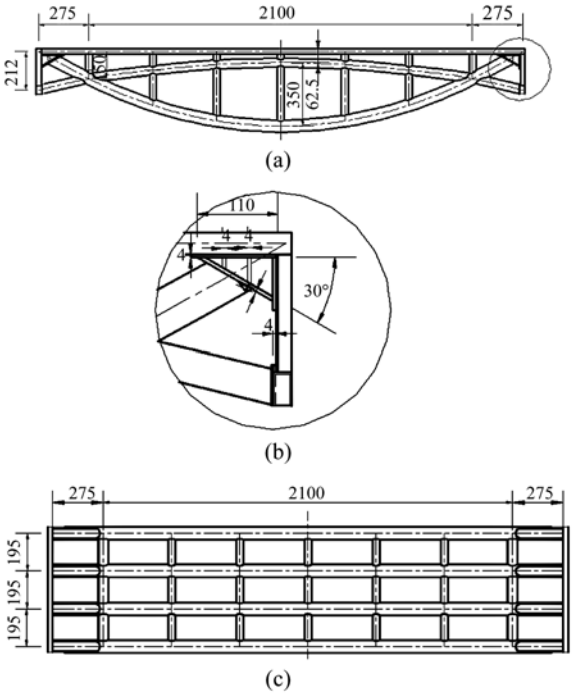

Fig.3 Dimension of the test model (unit: mm)
(a) Elevation; (b) Arch-spring joint details; (c) Plan

Table 1 Cross-section of the member

Members	Section type	D_t (mm)	D_g (mm)
Right arch	Circular tube	∅60×3.5	∅530×18
Invert arch	Circular tube	∅48×3.5	∅402×14
Chord	Rectangular tube	□50×30×2	□420×250×25
Web member	Circular tube	∅33×2.5	∅299×24
Brace system	Bar/rectangular tube	∅15, □40×20×2	∅180×12, □200×200×20

D_t: dimension of test model; D_g: dimension of full-scale gate

Table 2 Material properties

Dimension (mm)	f_y (N·m^2)	f_t (N·m^2)	δ (%)
∅60×3.5	245	430	20
∅48×3.5	255	425	29
∅33×3.5	265	425	21
∅16	375	795	38
Rectangular (□50×30×2)	275	395	29
Rectangular (□40×20×2)	295	415	26

f_y: yield strength; f_t: tensile strength; δ: elongation ratio

The test setup, as shown in Figs.4a and 4b, mainly included the gate slot, loading system of double-spring equalizing beam and supports. Gate slots were set at the two sides to grip the gate tightly, and rubber blankets were inserted between the gate slots and the model. The double-spring equalizing beam was composed of an equalizing beam and double-springs (Fig.4c). They simulated the application of load from both the water pressure (invert load) and the tidal bore shock (right load). Connected with the actuator, the equalizing beam and the double-springs spread the concentrated load all over the locations of the springs evenly to simulate uniform load. There were 42 double-springs over 42 locations. One spring of each double-spring was placed inside the equalizing beam and the other between the equalizing beam and the test model. A steel bar went through a double-spring and the double-spring was fixed with bolts on both ends of the steel bar. When the equalizing beam moved toward the model, the spring between the equalizing beam and the model would be compressed and the invert load was applied on the model. When the equalizing beam moved away from the model, the spring inside the equalizing beam would be compressed and the right load was applied on the model. In this way, the uniform load could be bilaterally applied on the gate.

The loading equipment was mechanics testing and simulation system (MTS) and the 1450 kN actuator was adopted.

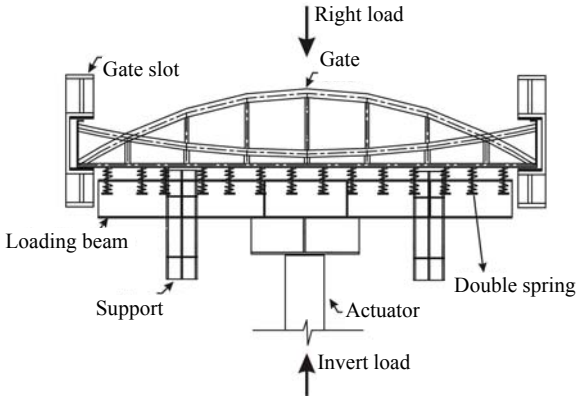

(a)

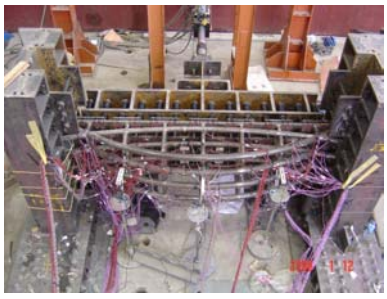

(b)

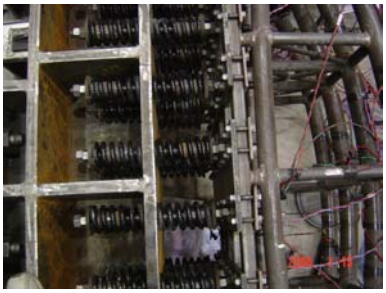

(c)

Fig.4 Test setup
(a) Loading system; (b) Test setup; (c) Spring system

Layout of measuring points

Approximately 120 channels for the strain gauges and rosettes were used to measure local responses (Fig.5). Two strain gauges were placed on each measuring point of arches and chords in order to measure axial strains. One was set on the side of the forward load and the other on the backward load side (The four pieces of the double-arch structure are sequenced from top to bottom as the first piece, the second piece, the third piece and the fourth piece). If a measuring point was labelled "*n*", the strain gauge on

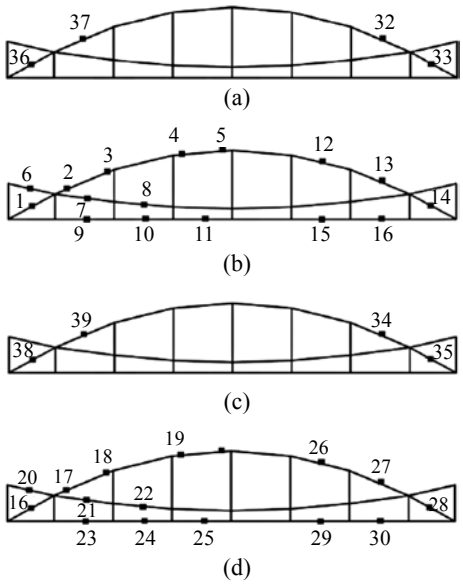

Fig.5 Layout of measuring points on the test
(a) The first piece; (b) The second piece; (c) The third piece; (d) The fourth piece

the forward load side would be labelled "n–1" and the other on the backward load side would be labelled "n–2". Strain rosettes were located at arch-springing joints (No. 2 joint) and the places where the main-arches and minor-arches were joined (No. 1 joint) (Fig.6). The global responses including the deflection were monitored by 5 displacement transducers along the span, three of which were placed respectively in the middle of the span, and the two placed where the main-arch and the minor-arch were joined. The other two were used to monitor the responses of the gate slots to offset slide. Electric resistance strain gauge and displacement transducers were used and the data from them were gathered automatically by the computer. Data were collected three times after each loading.

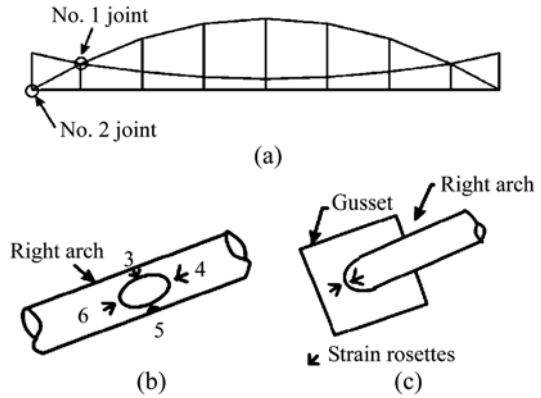

Fig.6 Location of strain rosettes

(a) Joints; (b) Strain rosettes located in joint No. 1; (c) Strain rosettes located in joint No. 2

Loading plan

Cyclic load was added step by step. Before the yield of structural members, the loading was controlled by the load. While after the yield of structural members, the loading was controlled by the displacement. The loading plan is shown in Table 3.

Table 3 Loading plan

Stage No.	Loading (kN)	Stage No.	Loading (kN)
1	–160~160	8	–380~380
2	–160~160	9	–410~410
3	–320~320	10	–410~410
4	–320~320	11	–440~440
5	–350~350	12	–440~440
6	–350~350	13	–470~470
7	–380~380	14	800

TEST RESULTS

Load-deflection curve

The load-deflection curve (Fig.7) shows: the cyclic curve is quite chubby, indicating good capacity of energy absorption; the structure has good ductility as it undergoes huge plastic deformation before complete damage. In addition, the structure has high bearing capacity as it still has certain rigidity after plastic deformation occurs.

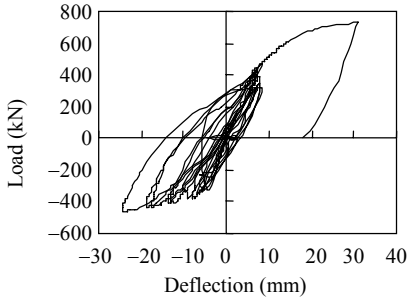

Fig.7 The deflection-load curve on the mid-span

Load-strain curve

The load-strain curves (Figs.8~11) also show: plastic deformation does not occur at the same moment for each member, which causes the differences

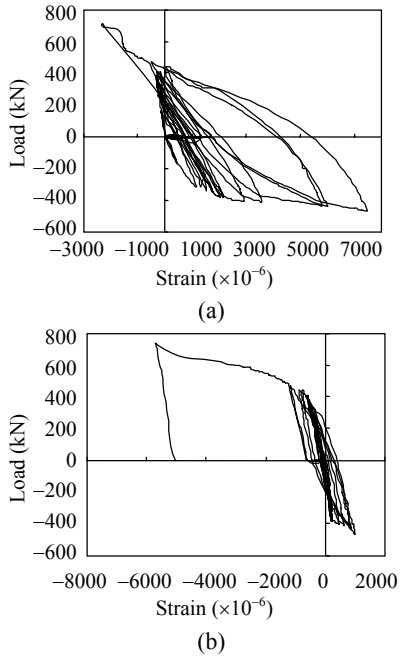

Fig.8 The load-strain curve of the principal strains 1 and 3 in the strain rosette No. 3 point

(a) Principal strain 1; (b) Principal strain 3

in their cyclic behaviors. The plastic strains of the rosette measuring points, located at No. 1 and No. 2 joints, are comparatively large, indicating they are the key parts of the structure.

Damage performance

Arch-springing joints (No. 2 joint) and the places where the main-arches and minor-arches are joined (No. 1 joint) get damaged. The gusset of No. 2 joint

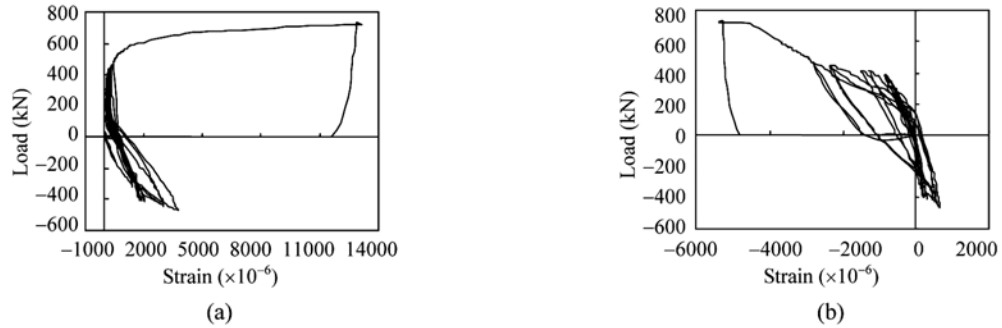

Fig.9 The load-strain curve of the principal strains 1 (a) and 3 (b) in the strain rosette No. 4 point

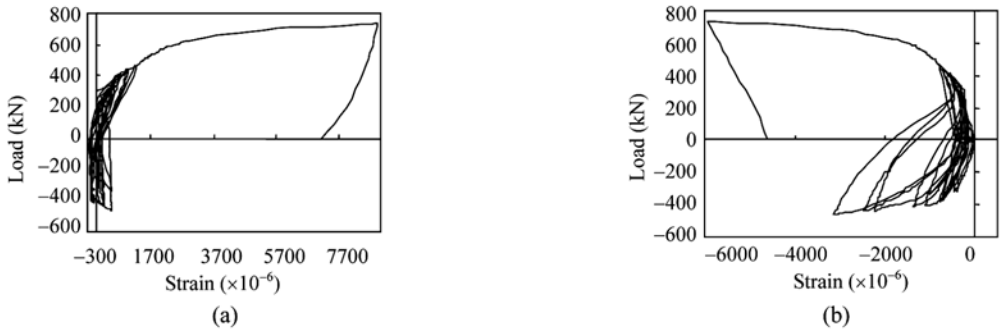

Fig.10 The load-strain curve of the principal strains 1 (a) and 3 (b) in the strain rosette No. 6 point

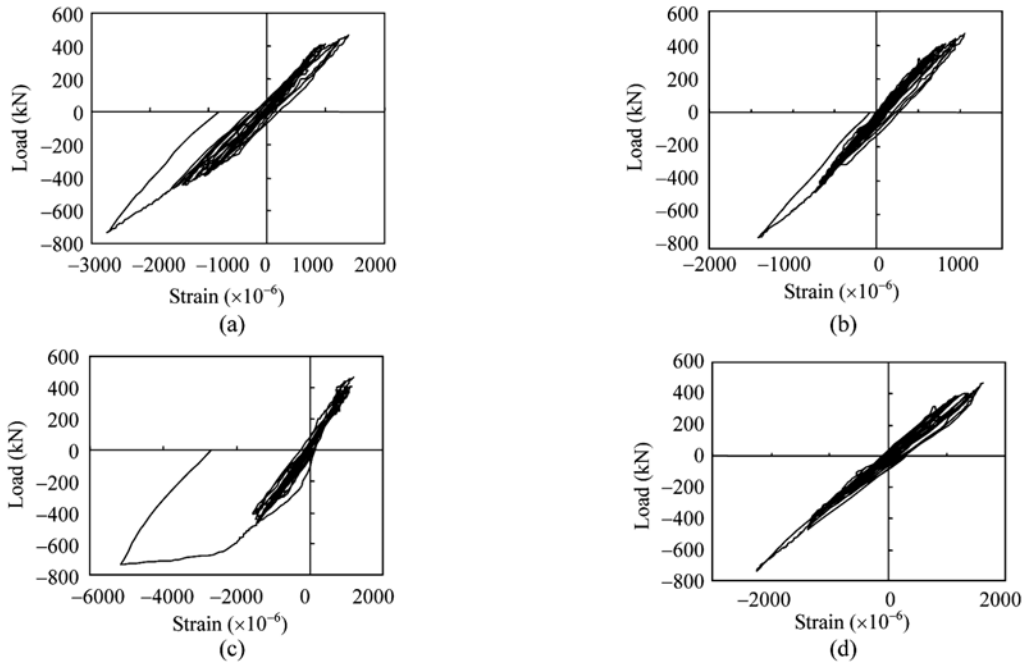

Fig.11 The load-strain curves. (a) Point 3-1; (b) Point 13-1; (c) Point 16-1; (d) Point 17-1

completely broke (Fig.12a) in the end, and the tube shell of the main arch of No. 1 joint became concave (Fig.12b). It proved them to be the weak as well as the key parts of the structure.

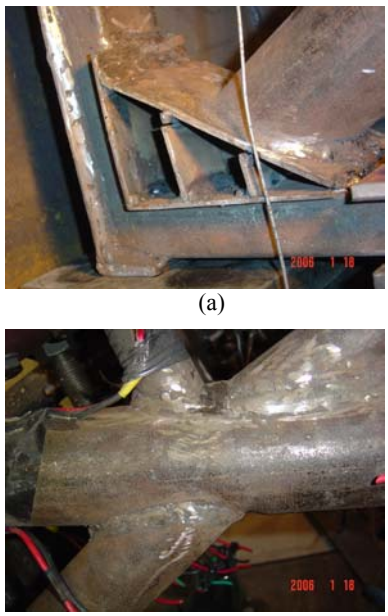

(a)

(b)

Fig.12 Damage of No. 2 joint (a) and No. 1 joint (b)

Analysis of bearing capacity

In the load-deflection figure, if a line is drawn to connect all the peak points of each cycle, the envelope curve of the cyclic curve can be obtained (Fig.13). Then the bearing capacity can be researched through the envelope curve accordingly (Aoki and Susantha, 2005).

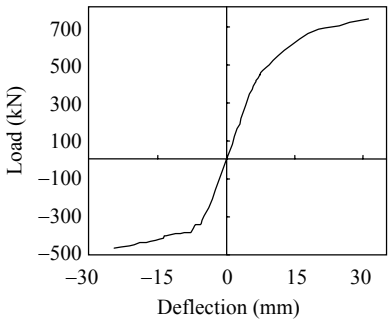

Fig.13 The envelope curve

The envelope curve shows that the bearing capacity of the structure under the right load is higher than that under the invert load. It can be explained as follows: when the arch-springing joint suffers damages, the right arch, which bears tension under the invert load, fails to be supported by the arch-springing joint. On the contrary, the right arch, which bears compression force under right load, can be supported by the arch-springing joint, and thus it can continue to bear load. This is also the reason why the tidal bore of the Qiantang River is designed to be the right load.

For further understanding of the bearing capacity of the gate, the envelope curve under the invert load is analyzed when the gate has low bearing capacity. The curve can be simplified as a bilinear line. It has a break when the load reaches −380 kN. At that moment, cracks are found in the arch-springing joints (No. 2 joint). Then 380 kN is regarded as the structural yield strength and the according point on the curve can be defined as the structural yield point.

The load-strain curve of the measuring point with the largest strain in the arch-springing joints is shown in Fig.14. The measuring point has already had residual plastic strain in the cycle when the load amplitude reaches 320 kN, although at that moment, the nominal test strain has not reached the yield strain of the material. It means there is much welding residual stress and stress concentration in the joints. The curve has no obvious yield point, so the concept of conditional yield point in material mechanics could be borrowed to define a "conditional yield point" (Sun and Hong, 1998) (Fig.14), The equation is shown below:

$$K_s = 0.7K_0, \tag{1}$$

where K_s stands for the secant modulus and K_0 stands for the initial tangent modulus. "Conditional yield point" can be regarded as the starting point when local plastic deformation occurs and is also defined as the local yield point in the load-deflection curve. Then the according load can be defined as the local yield strength, which is 200 kN.

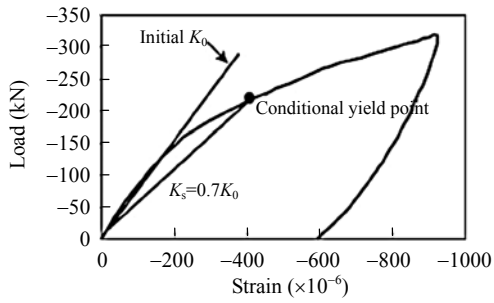

Fig.14 The load-strain curve in 320 kN amplitude cycle

The load-deflection curve is divided into three stages, the elastic stage, the local plastic stage and the failure stage, by local yield point and structural yield point (Fig.15). The loads for these two points are 200 kN and 380 kN, which are the local yield strength and structural yield strength respectively. Both are larger than the designing load, and thus the gate is safe enough for the projects. But there is much welding residual stress and stress concentration in the joints from the above analysis. It is harmful to the fatigue resistance of the structure.

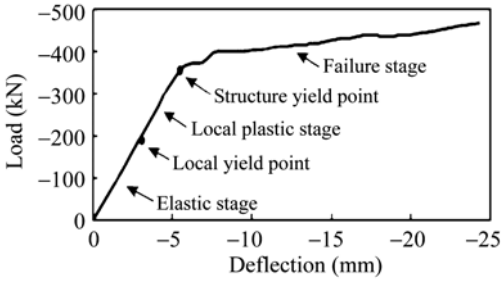

Fig.15 The characteristic of bearing capacity

Ductility capacities

The ductility can be researched through the envelope curve. The ductility factor is defined as follows:

$$\mu_{\Delta}=\Delta_{\mathrm{u}}/\Delta_{\mathrm{y}}, \tag{2}$$

where Δ_{u} is deflection of ultimate strength, Δ_{y} is deflection of structural yield strength. The ultimate strength of the gate model is not obtained in the test. The ductility factor can be analyzed as follows:

$$\mu \geq \Delta_{\max}/\Delta_{\mathrm{y}} = 4.8, \tag{3}$$

where $\Delta_{\max}$ is the biggest deflection in the test. From the expression, we can see that the gate meets the ductility requirement (AISC, 1999).

Property of joints

The above analysis showed No. 1 and No. 2 joints are the key and weak parts of the structure.

In order to evaluate the appropriateness of the joint design, the joint efficiency, defined as the ratio of the axial force of the member when the joints damage to the axial bearing capacity of the member (Chen and Shen, 2003), is calculated. For No. 2 joint, the joint efficiency is the ratio of the axial force of the right arch when the joints damage to the axial bearing capacity of the right arch. The joints are assumed to be damaged when the gusset breaks. For No. 1 joint, the joint efficiency is the ratio of the axial force of the invert arch when the joints damage to the axial bearing capacity of the invert arch. The joints are assumed to be damaged when the plastic deformation in the tube wall of the right arch exceeds 2% of the diameter. The efficiency of the two joints is low (Table 4). Meanwhile, it was found that there is much welding residual stress and stress concentration in the joints from the above analysis. It is harmful to the fatigue resistance of the structure. Therefore, the joints should be further researched and redesign.

Table 4 Efficiency of joint

Type	C_{j} (kN)	C_{w} (kN)	Efficiency (%)
No. 2 joint	85.0	152	55.9
No. 1 joint	58.4	125	46.7

C_{j}: Bearing capacity of joint; C_{w}: Bearing capacity of web member

DYNAMIC PROPERTY OF THE DOUBLE-ARCH GATE

The gate mainly bears dynamic loads such as tidal bore shock, so the analysis of the dynamic property is of significance. The FE model of the full-scale gate was built to analyze the dynamic property of the gate. The dimension of the model was eight times the dimension in Fig.3. The cross-sections of the members are shown in Table 1 and the thickness of the face plate was 14 mm. In the FE model, the beam element (ANSYS beam 188) was used to simulate the hollow steel tube and the shell element (ANSYS shell 181) was used to simulate the face plate of the gate. The FE model was composed of 14691 elements (Fig.16). Since the gate was mainly used to block the tide, the dynamic analysis studied

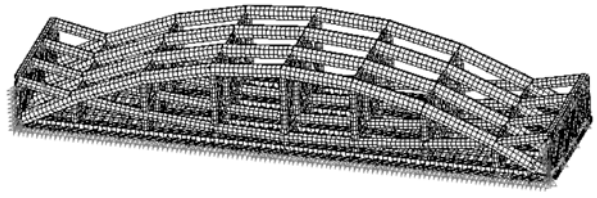

Fig.16 FEA model

the situation the minute the tide struck the gate. The two ends of the gate were restrained by the gate slots and the bottom of the gate was restrained by the floor when the gate was closed to block the tidal bore.

As a structure in water, the gate will inevitably interact with fluid. The fluid-structure interaction has been proven to be a very complex problem in hydro-kinematics and so far it has still not been completely solved (Qiu, 2004). A general way is to introduce additional mass of water into the dynamic equation of the structure. Let $\boldsymbol{M}_P$, $\boldsymbol{K}_P$ and $\boldsymbol{C}_P$ denote the mass, stiffness and damping matrices of the gate respectively, and $\boldsymbol{M}_s$, $\boldsymbol{K}_s$ and $\boldsymbol{C}_s$ denote the additional mass, additional stiffness and additional damping matrices caused by the fluid-structure interaction respectively. The dynamic equation is given as follows:

$$\boldsymbol{M}\ddot{\boldsymbol{X}} + \boldsymbol{C}\ddot{\boldsymbol{X}} + \boldsymbol{K}\boldsymbol{X} = F(t), \tag{4}$$

where $\boldsymbol{M}=\boldsymbol{M}_s+\boldsymbol{M}_P$, $\boldsymbol{C}=\boldsymbol{C}_s+\boldsymbol{C}_P$ and $\boldsymbol{K}=\boldsymbol{K}_s+\boldsymbol{K}_P$. To determine the natural vibration frequency of the structure, Eq.(4) can be simplified to:

$$\boldsymbol{M}\ddot{\boldsymbol{X}} + \boldsymbol{K}\boldsymbol{X} = \boldsymbol{0}, \tag{5}$$

in which only the effect of the additional mass $\boldsymbol{M}_s$ is taken into consideration in most cases.

Westergaard (1993) put forward a formula on additional mass caused by dynamic water stress:

$$P_w(h)=7\rho_w\sqrt{H_0 h}/8, \tag{6}$$

where H_0 is the water height, ρ_w is the density of the water, $P_w(h)$ is the additional mass of unit width at water height of h. Then the natural vibration frequencies of the gate under the normal water level on the Caoe River side (wet frequency) have been calculated (Table 5). Moreover, the natural vibration frequencies of the gate in air (dry frequency) have also been calculated (Table 5). It was found that each wet frequency is less than its corresponding dry frequency and that the minimum frequency of the gate in the wet mode is 7.08 Hz. The frequencies of the majority of the energy of tidal bore shock fall into the category of 0~2 Hz. Therefore the tidal bore shock will not cause resonance vibration of the gate.

Table 5 Natural vibration frequencies of the gate (Hz)

Mode	Dry frequencies	Wet frequencies
1	11.33	7.08
2	15.19	8.43
3	18.24	9.77
4	23.42	14.97
5	23.98	16.38
6	31.30	19.47
7	35.58	20.62
8	38.19	24.71
9	45.79	26.93
10	48.06	26.94

CONCLUSION

This paper mainly presents the cyclic behavior test of a scale model for the new double-arch steel gate functioning as tidal barrage and sluice in the Caoe River Dam. And we can draw the following conclusion.

(1) By studying the cyclic load-deflection curve of the gate, it was easy to find that the curve was a typical chubby rhomboid, and that the structure had good capacity of energy absorption and ductility.

(2) It could be found that arch-springing joints (No. 2 joint) and the places where the main-arches and minor-arches are joined (No. 1 joint) got damaged, so they were the weak and key parts of the gate and should be seriously considered.

(3) The bearing capacity characteristics of the gate were studied through the envelope curve, and it was found that the curve could be divided into three stages by the local yield point and the structural yield point: elastic stage, local plastic stage and failure stage. Both the local yield strength and structural yield strength were larger than the designing load, showing that the gate was safe enough for projects.

(4) The study showed that the joint efficiency of the two key joints was low. Moreover, it was found that there is much welding residual stress and stress concentration in the joints, which is harmful to the fatigue of the structure. Therefore, the joint should be further researched and redesigned.

(5) The dynamic property of the gate was analyzed by FEM considering the additional mass of water. It was found that the tidal bore shock would not cause resonance vibration of the gate.

References

AISC (American Institute of Steel Construction, Inc.), 1999. Load and Resistance Factor Design Specification for Structural Steel Buildings. AISC Committee, Chicago, p.180-181.

Alinia, M.M., Dastfan, M., 2007. Cyclic behaviors, deformability and rigidity of stiffened steel shear panels. *Journal of Constructional Steel Research*, **63**(4):554-563. [doi:10.1016/j.jcsr.2006.06.005]

Aoki, T., Susantha, K.A.S., 2005. Seismic performance of rectangular-shaped steel piers under cyclic loading. *Journal of Structural Engineering*, **131**(2):240-249. [doi:10.1061/(ASCE)0733-9445(2005)131:2(240)]

Billeter, P., Staubli, T., 2000. Flow-induced multiple-mode vibrations of gate with submerged discharge. *Journal of Fluids and Structures*, **14**(3):323-338. [doi:10.1006/jfls.1999.0274]

Chen, Y.Y., Shen, Z.Y., 2003. Experimental research on hysteretic property of unstiffened space tubular joint. *Journal of Building Structures*, **24**(6):57-62 (in Chinese).

Dong, S.L., Qiu, T., Luo, Y.Z., 2003. Spatial Structures. Jihua Press, Beijing, p.1-2 (in Chinese).

Ead, S.A., Rajaratnam, N., 1998. Double-leaf gate for energy dissipation below regulators. *Journal of Hydraulic Engineering*, **124**(11):1134-1145. [doi:10.1061/(ASCE)0733-9429(1998)124:11(1134)]

Elchalakani, M., Zhao, X.L., Grzebieta, R., 2003. Tests of Cold-Formed Circular Tubular Braces under Cyclic Axial Loading. *Journal of Structural Engineering*, **129**(4):507-514. [doi:10.1061/(ASCE)0733-9445(2003)129:4(507)]

Hsu, H.L., Shyu, Y.F., 2001. Cyclic responses of thin-walled structural steel members subjected to three-dimensional loading. *Thin-Walled Structures*, **39**(7):571-582. [doi:10.1016/S0263-8231(01)00016-7]

Kleiser, M., 1999. Steel lattice members under cyclic axial and flexural actions. *Journal of Structural Engineering*, **125**(4):393-400. [doi:10.1061/(ASCE)0733-9445(1999)125:4(393)]

Lin, F.J., Glauser, E.C., Johnston, B.G., 1970. Behavior of laced and battened structural members. *Journal of Structural Engineering*, **96**(7):1377-1401.

Mostafiz, R., Robert, L.H., 1996. Dynamic performance evaluation of gate vibration. *Journal of Structural Engineering*, **125**(4):445-452.

Qiu, L.C., 2004. Application of sponge layer method for radiation damping in analysis of dam-reservoir interaction. *Journal of Hydroengineering*, **58**(1):46-51 (in Chinese).

Sun, B.N., Hong, T., 1998. Elastic and Plastic Mechanics. Zhejiang University Press, Hangzhou, p.98-99 (in Chinese).

Westergaard, M., 1993. Water pressures on dams during earthquakes. *Trans. ASCE*, **9**(8):418-433.

Zhu, S.Z., 2005. The Scale-Model Test of the Hydraulic Steel Gate in Caoe River Dam. Report. Zhejiang University, Hangzhou, p.55-58 (in Chinese).